Long-life micro vacuum chamber for a micromachined cryogenic cooler

Haishan Cao,[a] Cristian H. Vermeer, Srinivas Vanapalli, Harry J. Holland, and H. J. Marcel ter Brake
Energy, Materials and Systems, Faculty of Science and Technology, University of Twente, 7500 AE Enschede, The Netherlands

(Received 4 May 2015; accepted 2 July 2015; published 17 July 2015)

Micromachined cryogenic coolers can be used for cooling small electronic devices to improve their performance. However, for reaching cryogenic temperatures, they require a very good thermal insulation from the warm environment. This is established by a vacuum space that for adequate insulation has to be maintained at a pressure of 0.01 Pa or lower. In this paper, the challenge of maintaining a vacuum chamber with a volume of 3.6×10^{-5} m^3 and an inner wall area of 8.1×10^{-3} m^2 at a pressure no higher than 0.01 Pa for five years is theoretically analyzed. The possible sources of gas, the mechanisms by which these gases enter the vacuum space and their effects on the pressure in the vacuum chamber are discussed. In a long-duration experiment with four stainless steel chambers of the above dimensions and equipped with a chemical getter, the vacuum pressures were monitored for a period of two years. In that period, the measured pressure increase stayed within 0.01 Pa. This study can be used to guide the design of long-lifetime micro vacuum chambers that operate without continuous mechanical pumping. © *2015 American Vacuum Society*.
[http://dx.doi.org/10.1116/1.4926961]

I. INTRODUCTION

Micromachined Joule–Thomson coolers have received increasing interest for applications that benefit from cryogenic temperatures and require a small cooling power ranging from a few milliwatts to hundreds of milliwatts.[1] Such applications include detectors in space missions,[2] low-noise amplifiers,[3] and high-temperature superconducting devices.[4] Micromachined cryocoolers need a vacuum insulation to minimize the parasitic loss that is due to the heat flow from the warm environment via the surrounding gas. To serve as an effective stand-alone micro cooling system, the microcooler and the device to be cryocooled need to be integrated in a micro vacuum chamber. As shown in Fig. 1, the heat load on the microcooler placed in a vacuum chamber includes the conduction of the surrounding gas and the radiation between the microcooler and the vacuum enclosure. In the free molecular flow regime, the conductive heat load increases with increasing chamber pressure. In the continuum regime, the effect of the chamber pressure on the conductive heat load is negligible. The microcooler is designed to withstand a heat load at the level of the radiation. The critical point, where the conductive heat load is equal to the radiative heat load, is typically at a pressure of about 0.01 Pa. Since both the radiation and conduction are proportional to the surface area of the microcooler, scaling the area has no effect on that critical-point pressure.

Two promising approaches to micro vacuum packaging have been presented, which are a component-level vacuum chamber and a wafer-level vacuum chamber.[5] A variety of fabrication techniques such as anodic bonding,[6] solder bonding,[7] glass frit bonding,[8] and getter techniques[8,9] have been investigated. However, so far only few researchers have paid attention to the testing of the lifetime of the micro vacuum chamber. Cheng *et al.*[7] demonstrated stable, long term testing of vacuum-packaged μ-resonators for 56 weeks at a pressure of 2.5 Pa which, as indicated above, is relatively high. Mitchell *et al.*[10] presented a vacuum packaging approach based on gold–silicon eutectic wafer bonding. The vacuum packages had a total volume of $2.3 \times 2.3 \times 0.9$ mm^3, in which micromachined Pirani vacuum sensors were encapsulated in order to measure the packaged pressures. With the use of getters and a prebond outgassing step, pressures can remain stable from about 0.5 to 3.1 Pa with measured pressure fluctuations within ± 0.3 Pa for four years. This paper addresses the issue of realizing a micro vacuum chamber to maintain pressure of 0.01 Pa or lower for at least five years.

II. THEORY

The increase in pressure of a vacuum chamber is due to the gases and vapors released from the chamber surface by means of various mechanisms. Such mechanisms involve internal and real leaks, vaporization, desorption, permeation, and diffusion.[11] Internal leaks such as gas pockets and real leaks caused by pathways through physical damages should and can be prevented by proper design and careful manufacturing. Vaporization is the gas flux caused by the sublimation of the chamber wall, feedthroughs, and other elements inside (microcooler and device to be cooled in our case). In dynamic equilibrium, the rate of molecules leaving the surface of the chamber wall equals the rate of molecules arriving at that surface. The pressure of the vapor in dynamic equilibrium is equal to the saturated vapor pressure of the chamber material. Most vacuum chamber materials (such as metal, glass, and ceramic) at ambient temperatures have saturated vapor pressures that are orders of magnitude smaller than the required vacuum pressure of about 0.01 Pa. Therefore, when using the right materials, the effect of vaporization can be neglected in the design. The other three

[a]Electronic addresses: H.Cao@utwente.nl; HaishanCao@gmail.com

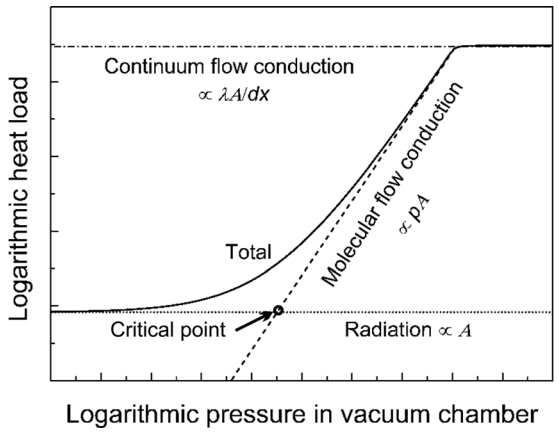

FIG. 1. Heat load on a microcooler vs pressure in a vacuum chamber.

causes of pressure increase namely desorption, permeation, and diffusion are subsequently considered in Secs. II A–II C.

A. Desorption

Desorption is the release of adsorbed adsorbates from the surface of the adsorbent. These adsorbates can result from direct adsorption or from the final step in a permeation process. The rate of desorption is a function of the molecular binding energy between the adsorbent and the adsorbate, the surface temperature, and the surface coverage. When the internal surface of a vacuum chamber is exposed to air, the surface will be covered with layers of water molecules. A pump-down process of a vacuum chamber starting from atmospheric pressure goes through two stages. To begin with, the dry air is mostly pumped away. And after that, the water molecules desorbing from the internal surfaces follow. Once the pressure inside is around 0.01 Pa, the desorbing water makes up over 99% of the total gas load.[12] The outer layers of water on the surface are adsorbed physically and the physisorbed water can be removed quickly when the pressure around the surface is lower than 2300 Pa, which is the saturated vapor pressure of water at ambient temperature of 293 K.[13] The innermost layer of water has a chemical binding and is difficult to remove at ambient temperature. Water adsorption and desorption on various material surfaces (including steel, aluminum, copper, glass, Teflon, and polyvinyl chloride) were studied by R Dobrozemsky using the tritium-tracer technique.[14,15]

Consider a vacuum chamber of which the wall surface is covered with a monolayer of water molecules. Then, the conservation of mass results in[16]

$$V\frac{dp}{dt} + Sp + A\frac{dN}{dt}k_BT = 0, \tag{1}$$

where V is the inner volume of the chamber (m^3), p is the pressure in the chamber (Pa), S is the pumping speed ($m^3\ s^{-1}$), A is the inner area of the chamber (m^2), N is the surface density of water molecules (molecules m^{-2}), and k_B is the Boltzmann constant.

The desorption rate of water can be expressed as a first-order reaction

$$-\frac{dN}{dt} = \frac{N}{\tau_0}\exp\left(-\frac{E}{RT}\right), \tag{2}$$

where τ_0 is the nominal period of vibration of the bond between the adsorbed molecule and the substrate which is usually taken to be about 10^{-13} s,[17] and E is the activation energy of desorption (J mol^{-1}). Equation (2) shows that pumping will be more effective at a higher temperature.

During a pumpdown, the desorption rate is initially high due to the fact that the outer layers of water on the surface have weaker water to water bonds (4.2×10^4 J mol^{-1}),[17] and break easily. The innermost layer of water has much higher bond energies and desorbs much more slowly. The activation energy of desorption of the innermost layer of water on stainless steel is in the range of 1.00×10^5–1.07×10^5 J mol^{-1}, which is dependent on the surface coverage.[18] According to R Dobrozemsky's experimental data,[14,15] the virtual energy of desorption of water on glass is also in this range.

When pumping is stopped then Eq. (1) shows that the increase in pressure is given by

$$\frac{dp}{dt} = -\frac{dN}{dt}\frac{A}{V}k_BT. \tag{3}$$

This equation shows that a smaller volume will cause a faster pressure increase for a given surface area. This means that it is more difficult for a chamber with a larger surface to volume ratio to maintain a constant pressure level. This is the case for microcoolers since area scales with size[2] and volume with size.[3] Thus, if size goes down, A/V increases.

We assume that, when pumping is stopped, only the innermost layer of water is left on the surface. A water molecular diameter of 0.3 nm then results in a molecule density N_0 of 10^{19} molecules m^{-2}. Equation (3) can be used to derive the relation between pressure and molecule density after pumping has been stopped as

$$(p - p_0) = \left(\frac{Ak_BT}{V}\right)(N_0 - N). \tag{4}$$

Based on Eq. (2), the surface density of water molecules with an initial value, N_0, after a certain time, t, becomes

$$N = N_0\exp\left(-\alpha\frac{t}{\tau_0}\right), \quad \text{where } \alpha = \exp\left(-\frac{E}{RT}\right). \tag{5}$$

By combining Eqs. (2) and (5), the desorption rate of the innermost layer of water with molecular surface density, N_0, can be obtained. Figure 2 shows the desorption rates of water with various activation energies of desorption and with $N_0 = 10^{19}$ molecules m^{-2}. As can be expected, the desorption rate of water with lower activation energy is higher at the start and decreases faster than that of water with higher activation energy.

While N decreases in time, p increases. Assume we stop pumping at a very low pressure (i.e., $p_0 = 0$) and furthermore that after pumping is stopped, all remaining molecules at molecule density N_0 desorb, and thus, build up pressure.

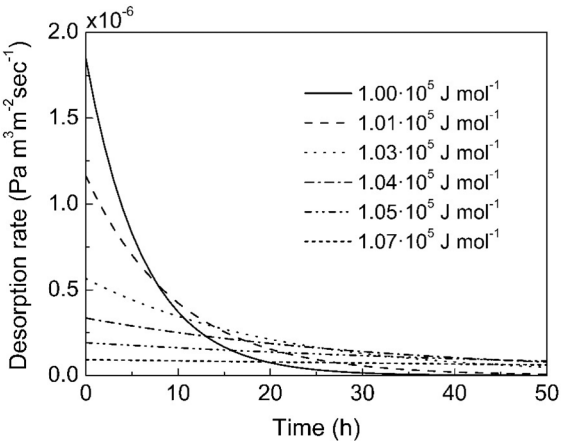

FIG. 2. Desorption rate of water molecules as a function of time with different activation energies with initial molecular surface density of 10^{19} molecules m^{-2} at ambient temperature.

Then, according to Eq. (4), the resulting pressure in the chamber is

$$p = \frac{Ak_BT}{V}N_0. \tag{6}$$

Consider a microcooler vacuum chamber with inner volume V of 3.6×10^{-5} m^3, inner area A of 8.1×10^{-3} m^2, and resulting surface area-to-volume ratio of $225\,m^{-1}$. The considered vacuum chamber has the same geometry as the vacuum chamber that is described and discussed in Sec. IV. Equation (6) yields the end pressure of $p = 9$ Pa at ambient temperature, as indicated in Fig. 3 that shows the pressure increase in the chamber after pumping is stopped as a function of time with different activation energies.

If we want a vacuum space to remain at a pressure below a maximum p^*, then Eq. (6) shows that we need to reduce the molecule density to N^*

$$N^* = \frac{p^*V}{Ak_BT}. \tag{7}$$

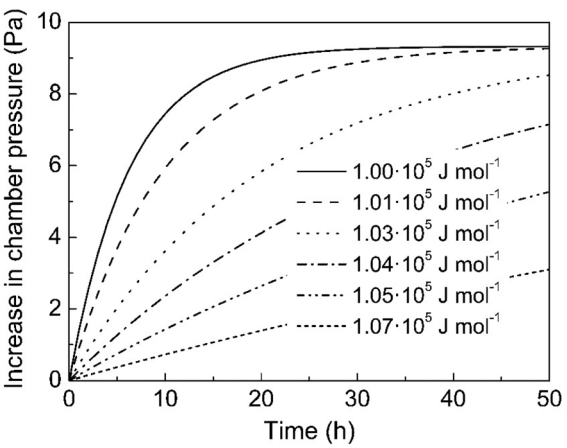

FIG. 3. Increase in chamber pressure due to desorption after pumping is stopped as a function of time at various activation energies. Chamber volume 3.6×10^{-5} m^3, inner area 8.1×10^{-3} m^2, and initial molecular surface density 10^{19} molecules m^{-2} at ambient temperature.

Equation (5) shows that the pumping time required to arrive at this molecule density is given by

$$t^* = \frac{\tau_0}{\alpha}\ln\frac{N_0}{N^*}. \tag{8}$$

Since $\alpha = \exp(-E/RT)$, it is again clear that pumping at an elevated temperature is beneficial.

Figure 4 shows the relationship between the required bake-out time as a function of the baking temperature at various activation energies. As shown in Fig. 4, it is hard to remove the chemisorbed water at ambient temperature, but water molecules are easily desorbed by baking at about 100 °C.

B. Permeation

Permeation is a three-stage process, consisting of the adsorption of gases at the exterior surface of the vacuum-chamber wall, the diffusion through the wall, and the desorption at the interior surface. In general, the diffusion through the wall determines the dynamics and the problem is described by the diffusion equation. For a stainless steel chamber, hydrogen gas is the most relevant diffusing gas, accounting for 90% or more of the permeation.[19] Helium gas permeation is dominant in case of a glass vacuum chamber.[20] The permeation of hydrogen gas in a stainless steel chamber and that of helium gas in a glass chamber are analyzed below.

It is assumed that the chamber wall has been completely degassed, which means that the gas concentration c inside the chamber wall is initially zero. This can only be realized if the micro vacuum chamber as a whole is placed in a larger vacuum oven. At time $t = 0$, the micro vacuum chamber is closed, it is taken out of the vacuum oven, and the outer surface is exposed to air. Then, this exposure produces a concentration c_1 at this outer surface and the inner surface is maintained under vacuum.

According to Sievert's law, the concentration on the outer surface is given by[20]

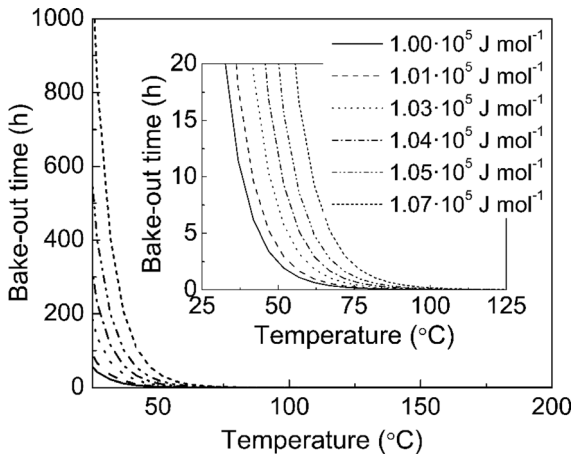

FIG. 4. Bake-out time determined by desorption process as a function of baking temperature with different activation energies. Chamber volume 3.6×10^{-5} m^3, inner area 8.1×10^{-3} m^2, and initial molecular surface density 10^{19} molecules m^{-2}.

$$c_1 = \frac{K}{D} p_1^n, \tag{9}$$

where D is the diffusivity, K is the permeability, and p_1 is the partial pressure of the gas under consideration. The partial pressures of hydrogen and helium gas in normal air are 0.055 and 0.520 Pa, respectively. In the case of permeation of hydrogen gas through metals, $n = 0.5$. For the permeation of helium gas through dielectrics such as glass, $n = 1$.[20]

It has been well established that the diffusivity and permeability of hydrogen gas in metals are given by Arrhenius-type equations

$$D = D_0 \exp(-E_d/RT), \tag{10}$$

$$K = K_0 \exp(-E_k/RT). \tag{11}$$

For diffusivity, the values of the constant D_0 and the thermal activation energy E_d of hydrogen gas in 304 type steel are 4.7×10^{-7} m^2 s^{-1} and 5.4×10^4 J mol^{-1}, respectively. For permeability, the values of the constant K_0 and the thermal activation energy E_k of hydrogen gas in 304 type steel are 1.9×10^{-4} Pa$^{0.5}$ m^3 m^{-1} s^{-1} and 6.0×10^4 J mol^{-1}, respectively, as reported by Louthan and Derrick.[21]

Perkins[20] proposed formula that fit the diffusivity and permeability data for helium gas in glass (vitreous silica) as

$$D = D_T T \exp(-E_d/RT), \tag{12}$$

$$K = K_T T \exp(-E_k/RT), \tag{13}$$

where D_T is 3.0×10^{-11} m^2 K^{-1} s^{-1}, E_d is 2.0×10^4 J mol^{-1}, K_T is 2.1×10^{-13} m^2 K^{-1} s^{-1}, and E_k is 1.8×10^4 J mol^{-1}.

The one-dimensional diffusion equation is

$$D \frac{\partial^2 c}{\partial^2 x} = \frac{\partial c}{\partial t}. \tag{14}$$

The maximum permeation rate will occur if the inside concentration is assumed to remain zero. Then, considering a wall of thickness d and $x = 0$ at the inner surface, the initial and boundary conditions are $c(x,0) = 0$; $c(0,t) = 0$; and $c(d,t) = c_1$.

The solution to the diffusion equation is[22]

$$c(x,t) = \frac{xc_1}{d} + \frac{2c_1}{\pi} \sum_{n=1}^{\infty} \frac{(-1)^n}{n} \times \sin\left(\frac{n\pi x}{d}\right) \exp\left(-\left(\frac{n\pi}{d}\right)^2 Dt\right). \tag{15}$$

The instantaneous permeation rate (Pa m^3 m^{-2} s^{-1}) at the interior surface at time t is

$$\dot{Q}(t) = D\left(\frac{\partial c}{\partial x}\right)_{x=0} = \frac{Dc_1}{d} + \frac{2Dc_1}{d} \sum_{n=1}^{\infty} (-1)^n \exp\left(-\left(\frac{n\pi}{d}\right)^2 Dt\right). \tag{16}$$

The steady-state permeation rate is

$$\dot{Q}_p(\infty) = \frac{Dc_1}{d}. \tag{17}$$

The time to reach this steady state can be approximated by t_c which is known as the critical time and is given by[23]

$$t_c = \frac{d^2}{6D}. \tag{18}$$

For the permeation of helium gas through a 2 mm thick glass chamber, the critical time is only about 2 days. Thus, in practice the permeation rate of helium gas through a glass chamber can be considered to be at the steady-state rate.

The permeation of hydrogen gas through a 2 mm thick stainless steel chamber has a critical time of more than 100 years. As the thickness decreases from 2 to 0.2 mm, the critical time decreases from about 100 years to one year.

Figure 5 shows the relationship between the steady-state permeation rate and the wall thickness of the vacuum chamber. The steady-state permeation rate of hydrogen gas through a stainless steel chamber wall is about 1 order of magnitude lower than that of helium gas through a glass chamber (for the same wall thickness).

The actual permeation rate of helium gas through a glass chamber in a period of five years can very well be approximated by its steady-state rate due to its short critical time. The actual permeation rate of hydrogen gas through a stainless steel chamber, in general, is smaller than its steady-state rate. The actual permeation rate of hydrogen gas through a stainless steel chamber can be evaluated by Eq. (16) and is shown in Fig. 6(a) for a period of five years. As shown in Fig. 6(a), the actual permeation rate increases with time, gradually approaching its steady-state permeation rate. Furthermore, the actual permeation rate decreases rapidly with increasing wall thickness. The pressure built up in a period of five years in the stainless steel vacuum chamber with different thicknesses (volume 3.6×10^{-5} m^3 and inner area 8.1×10^{-3} m^2), due to the permeation of hydrogen gas, is shown in Fig. 6(b). The resulting pressure built up is lower

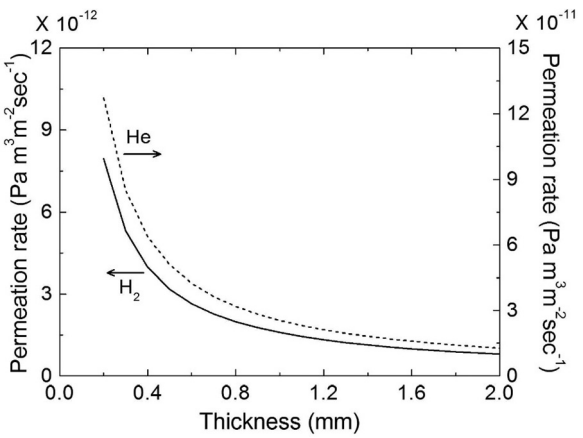

FIG. 5. Steady-state permeation rate as a function of wall thickness of stainless steel and glass vacuum chamber for hydrogen and helium gas, respectively, with corresponding partial pressures of 0.055 and 0.52 Pa.

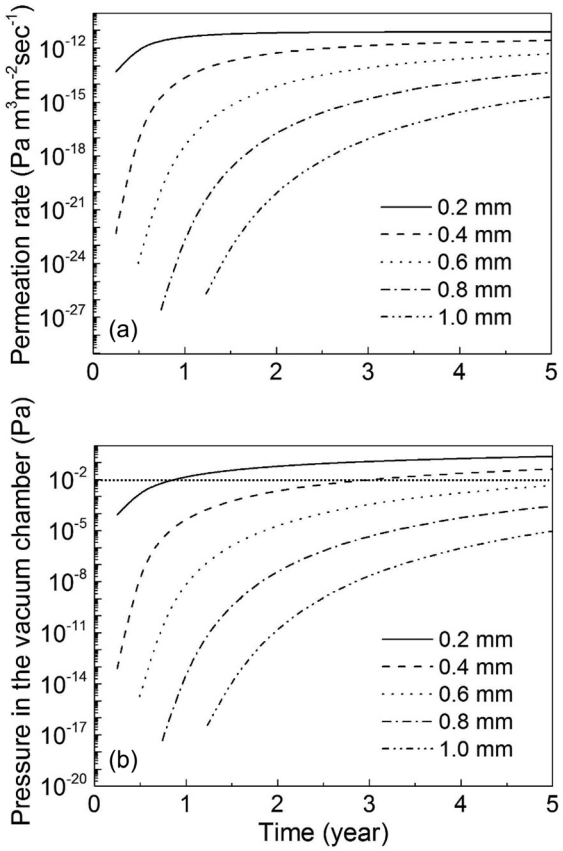

FIG. 6. (a) Permeation rate of hydrogen gas through stainless steel vacuum chamber wall with different wall thicknesses as a function of time. (b) Pressure built up in stainless steel vacuum chamber with different wall thicknesses (volume 3.6×10^{-5} m^3 and inner area 8.1×10^{-3} m^2) due to permeation of hydrogen gas in a period of five years.

than the microcoolers' acceptable vacuum pressure (0.01 Pa) when the wall thickness is larger than 0.6 mm. In contrast, the pressure built up in a glass vacuum chamber due to helium gas permeation quite quickly reaches this acceptable level. Figure 5 shows that at a thickness of about 2 mm, the helium gas permeation rate is around 1.5×10^{-11} Pa m^3 m^{-2} s^{-1}. With the above mentioned values for area and volume, a pressure of 0.01 Pa is reached in about one month. The permeation of helium gas through glass can be limited by coating it with titanium.[24] Besides functioning as a permeation barrier, titanium also absorbs other residual gases such as water and oxygen.

Glass and ceramics are widely used for optical and electrical feedthroughs. It is extremely important that these feedthroughs have a low helium-gas permeation rate in order to establish a long lifetime micro vacuum chamber. The leak rate of a commercial electrical feedthrough[25] was measured in an environment with a helium gas pressure of 10^5 Pa to be lower than 10^{-11} Pa m^3 s^{-1}. Therefore, the helium gas leak rate in normal air with a helium gas partial pressure of 0.52 Pa should be less than 5.2×10^{-17} Pa m^3 s^{-1}. For the chamber discussed above with an internal volume of 3.6×10^{-5} m^3, pressure level of 0.01 Pa, and lifetime of five years, the acceptable pressure increase rate is 2.3×10^{-15} Pa m^3 s^{-1}. Thus, the helium leak rate of feedthroughs for the discussed chamber is acceptable. Perkins[20] pointed out that the permeability of CGW 1720 (Pyrex) glass is of the same order of magnitude as that of the 97% alumina ceramic (no data were reported as to the over-all composition), when the application temperature is less than 200 °C. Compared to Corning 9606 pyroceram (a glass ceramic) and mullite ceramic in the temperature range less than 200 °C, the permeability of CGW 1720 glass and the 97% alumina ceramic is much lower. Thus, the application of the latter two materials as insulators of feedthroughs is attractive in vacuum-chamber applications.

C. Diffusion

The outgassing in a vacuum chamber due to permeation is caused by the gases from the outside of the vacuum chamber. Except for the outside gases, also gases in materials inside the vacuum chamber contribute to the system outgassing through diffusion.

Consider a material with thickness d and initial gas concentration c_1 that is placed in a vacuum environment at $t=0$. Then, the initial and boundary conditions in the diffusion process are $c(x,0) = c_1$; $c(0,t) = 0$; and $c(d,t) = 0$.

The solution is[22]

$$c(x,t) = \frac{4c_1}{\pi}\sum_{n=0}^{\infty}(2n+1)^{-1}\sin\frac{\pi(2n+1)x}{d} \times \exp\left(-\left(\frac{\pi(2n+1)}{d}\right)^2 Dt\right). \tag{19}$$

The instantaneous outgassing rate at the surface $x=0$ is

$$\dot{Q}(t) = D\left(\frac{\partial c}{\partial x}\right)_{x=0} = \frac{4c_1 D}{d}\sum_{n=0}^{\infty}\exp\left(-\left(\frac{\pi(2n+1)}{d}\right)^2 Dt\right), \tag{20}$$

where D again is the diffusivity. At relatively large values of the time t, the contributions of the subsequent terms in the series of Eq. (20) decrease very rapidly. If $Dt/d^2 > 0.029$ then the second term is 10% of the first and the third is only 1% of the second. Therefore, if $Dt/d^2 > 0.029$ we can approximate the outgassing rate as

$$\dot{Q}(t) = \frac{4c_1 D}{d}\exp\left(-\left(\frac{\pi}{d}\right)^2 Dt\right). \tag{21}$$

To reduce the outgassing rate through diffusion, a baking process is usually adopted before the vacuum chamber is sealed. The objective of the bake-out process is to degas the wall of the vacuum chamber and all materials inside the chamber. The required bake-out time of hydrogen in a stainless steel chamber and that of helium in a glass vacuum chamber can be approximated using Eq. (21). Assume that when the baking and pumping is stopped, the outgassing continues at a constant rate as expressed by Eq. (21). Then the pressure built up in a certain time interval can be

evaluated by multiplying the time elapsed with the outgassing rate and area/volume (outgassing rate is in Pa m^3 m^{-2} s^{-1}). In other words, the acceptable outgassing rate is determined by required pressure, lifetime, and the surface area-to-volume ratio of the vacuum chamber. Considering the wall of the chamber discussed above with an internal volume of 3.6×10^{-5} m^3, inner area 8.1×10^{-3} m^2, pressure level of 0.01 Pa, and lifetime of five years, the resulting acceptable outgassing rate is 2.8×10^{-13} Pa m^3 m^{-2} s^{-1}. The diffusivity D is a function of the thermal activation energy of the diffusing gas in the solid as expressed in Eqs. (10) and (12). Because of the exponential dependence on temperature, an increase in temperature will sharply increase the diffusivity and reduce the required bake-out time. With the given acceptable outgassing rate of 2.8×10^{-13} Pa m^3 m^{-2} s^{-1}, the bake-out time of hydrogen in case of the wall of a stainless steel chamber and that of helium in the wall of a glass vacuum chamber both for an interval of five years and a pressure built up of 0.01 Pa are depicted in Fig. 7. The initial hydrogen concentration in stainless steel and helium concentration in glass are related to their partial pressures in air by means of Sieverts' law,[20] $c_1(H_2) = 8.55$ Pa m^3 m^{-3} and $c_1(He) = 8.1 \times 10^{-3}$ Pa m^3 m^{-3}. Due to the stainless steel and glass production procedure, the amounts of hydrogen and helium dissolved in the two types of material can be higher than the value evaluated based on Sieverts' law. However, the initial concentration value does not influence the baking time a lot because the baking time is much more determined by the material thickness d and the diffusivity D as indicated by Eq. (21).

As shown in Fig. 7, the bake-out time decreases rapidly with increasing bake-out temperature. Furthermore, the bake-out time can be decreased significantly by reducing the material thickness. However, a thinner wall increases the permeation rate. As shown in Fig. 6, a stainless steel wall requires a thickness of 0.6 mm and Fig. 7 shows that in that case a bake-out at, e.g., 350 °C for 18 h is adequate. Compared to the bake-out time required for stainless steel, the bake-out time required for glass is much shorter, which means that the diffusion resistance of helium through glass is smaller. The smaller diffusion resistance also implies that the outgassing due to permeation of helium through glass is an issue as discussed in Sec. II B, and a permeation barrier, such as a titanium film, is needed.

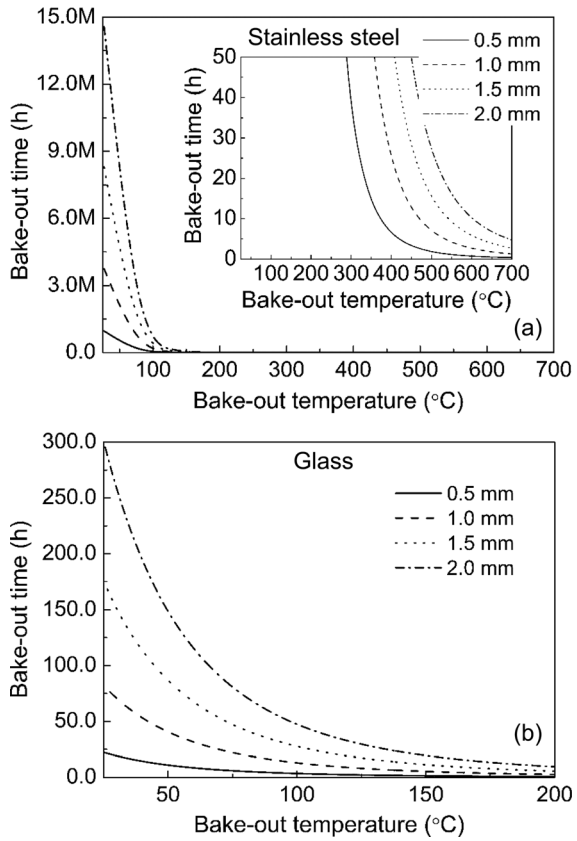

FIG. 7. Bake-out time required for stainless steel (a) and glass vacuum (b) chamber walls with different wall thicknesses (volume 3.6×10^{-5} m^3 and inner area 8.1×10^{-3} m^2) as a function of bake-out temperature, based on acceptable pressure built up due to remaining hydrogen or helium outgassing of 0.01 Pa in five years.

III. GETTER PUMPS

As shown above, the bake-out time can be strongly reduced by increasing the bake-out temperature. However, electronic devices inside the vacuum chamber and other components may limit the maximum bake-out temperature which may result in insufficient baking. Getter pumps[26] are commonly used in these vacuum chambers to provide a long-term pumping mechanism after the chambers are sealed. Getter pumps include evaporable getters[27] and nonevaporable getters.[28] Evaporable getters employ volatile and reactive materials such as barium and titanium,[29] which are heated, evaporated, and deposited on adjacent surfaces. These deposited materials capture gases on their surface in the form of stable chemical compounds. The pumping speed of an evaporable getter depends on the sticking coefficient of the gas on the surface. The sticking coefficient is higher at lower temperatures. In contrast, nonevaporable getters adsorb gases at the surface, followed by diffusion of gases into the getter material. As indicated by name, the materials used in nonevaporable getters remain in the solid state instead of being evaporated and deposited on a surface. The pumping speed of a nonevaporable getter is

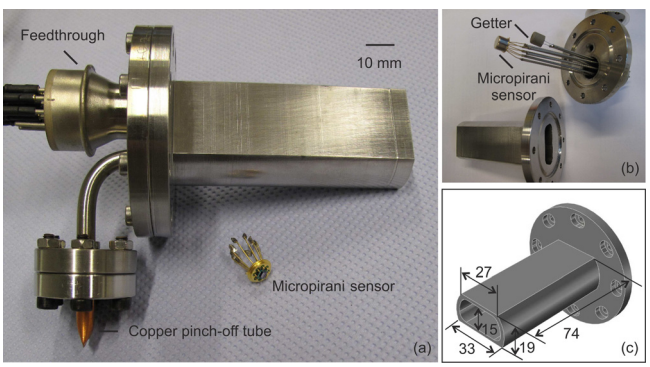

FIG. 8. (Color online) (a) Photograph of the micro vacuum chamber. (b) Two separate parts of the micro vacuum chamber. (c) Geometry of the chamber (dimensions in mm).

TABLE I. Overview of the set of measurements.

Chamber	Cleaning	Baking chamber 550 °C[a]	Baking total 100 °C[b]	Pump during activation	Getter activation temperature (°C)
1	X	X	X	X	900 (5 min)
2	X	X	X	X	450 (30 min)
3	X	X		X	450 (30 min)
4	X		X	X	450 (30 min)

[a]The baked chamber (without feedthrough, copper pinch-off tube, getter and pressure sensor) is in a vacuum oven at a pressure 1 Pa. The temperature inside ramps up to 550 °C from ambient temperature at 25 °C h^{-1} and remains stable at 550 °C for 56 h, then cools down to ambient temperature at 17.5 °C h^{-1}. After baking, the chamber is exposed to air for half an hour before assembling with flange cover.

[b]The assembled vacuum chamber is baked at 100 °C for 22 h connected with a turbo molecular pump at a pressure of less than 10^{-4} Pa.

limited by the diffusion process.[11] Since an increase in temperature represents an increase in the average molecular speed, the diffusion rate increases with increasing temperature. The getter pumps used in the experiment, discussed in Sec. IV, are nonevaporable getters that employ a porous, sintered, zirconium alloy.[30,31] The getter can sorb hydrogen, carbon monoxide, carbon dioxide, oxygen, nitrogen, and water vapor at room temperature. Hydrocarbons are sorbed only at temperatures around 300 °C. Noble gases cannot be sorbed by this kind of getter. To capture noble gases or hydrocarbons at room temperature, the getter must be used in combination with a second pump, most commonly a sputter-ion pump.[32]

IV. EXPERIMENTAL RESULTS AND DISCUSSION

The effect of baking and getter activation was investigated with a micro stainless steel vacuum chamber with a wall thickness of 2 mm [shown in Fig. 8(a)]. Sealing between two separate parts of the micro vacuum chamber, shown in Fig. 8(b), is achieved by putting a copper gasket in between them. Figure 8(b) also shows the electrical connections of the micropirani sensor and the getter to the electrical feedthrough. Figure 8(c) shows the geometry of the chamber without a cap, in which the cross section of the chamber is included. The cleaning procedures for the vacuum chambers included: remove all debris by blowing out with a high-pressure nitrogen line, wash in a hot water jet (approximate 80 °C), dry using a clean high-pressure nitrogen flow, clean using acetone in an ultrasonic bath for at least 30 min, dry using clean high-pressure nitrogen flow, clean using isopropanol in an ultrasonic bath for at least 30 min, and finally, dry using clean high-pressure nitrogen flow. The inner volume and area are 3.6×10^{-5} m^3 and 8.1×10^{-3} m^2 respectively. An electrical feedthrough with 10 pins was used in the measurements.[25] The pin header feedthrough is an alumina ceramic feedthrough with a helium gas leak tightness less than 5.2×10^{-17} Pa m^3 s^{-1}. To minimize outgassing rates, a small manometer with little material and a low outgassing rate is necessary. A micropirani sensor kit (calibrated for nitrogen at 25 °C) was chosen.[33] In addition, an ST172 nonevaporable getter of SAES Getter was integrated in the chamber.[34]

A total of four micro vacuum chambers were prepared. Table I presents an overview of the baking process of these chambers as well as the getter activation temperature.

After the cleaning and baking steps, the copper pinch-off tubes of the vacuum chambers are pinched off and from that moment the pressures inside the chamber were recorded. Because the fourth chamber was not baked at a higher temperature, the measurement started seven days earlier than for the other chambers, as shown in Fig. 9. Compared to the other three chambers, only the third assembled chamber was not baked at 100 °C. Figure 9 shows that the pressure in the third chamber gradually increases to about 0.15 Pa in the first 60 days because the desorption rate of water molecules of the third chamber is higher than the pumping rate of the SAES Getter. This indicates that baking the assembled chamber at 100 °C is necessary because the water layer forms again after a short time once the baked stainless steel chamber is exposed to atmospheric air.[35,36] The pressure in the third chamber decreases after 60 days because the desorption rate of water drops below the gettering rate. This matches the prediction shown in Fig. 4 that baking at a temperature of 100 °C is high enough to desorb water molecules. No difference was observed between activation of the getter at 450 °C for 30 min and 900 °C for 5 min (chambers 1 and 2). The pressures in chambers 1 or 2, and 4 increase from the zero setpoint to

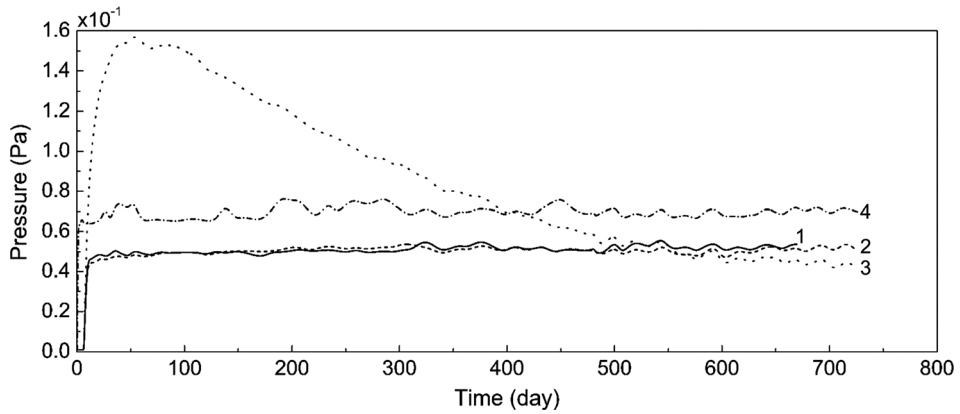

FIG. 9. Pressures in stainless steel vacuum chambers vs time.

about 0.05 and 0.07 Pa, respectively, in few hours as indicated in Fig. 9. This is caused by a temperature-offset effect of the pressure transducers. These transducers were set to zero being still at a relatively high temperature after completing the baking process and pinching off the tubes. As the temperature decreased to ambient level, the outputs increased. Correcting for these offsets, we can conclude that in the period of two years the pressure increase is below 0.01 Pa. This implies that the pressure does not increase due to the permeation or diffusion of hydrogen gas, although this does not directly verify the predictions presented in Secs. II B and II C, because a getter has to be used in the vacuum chamber under test, which is not considered in the simulation.

V. CONCLUSIONS

In this paper, the establishment of a vacuum in small-sized vacuum chambers is studied. The possible sources of gas, the mechanisms by which these gases enter the vacuum space, and their effects on the vacuum level are discussed theoretically. As an illustrative case, a vacuum chamber with a volume of 3.6×10^{-5} m^3 and an inner wall area of 8.1×10^{-3} m^2 is assumed. Stainless steel and glass are considered as the wall materials. Furthermore, we assume a pressure increase to a level of 0.01 Pa in a period of five years to be the acceptable limit. In the vacuum pumping procedure, it is difficult to remove the monolayer chemisorbed water on the stainless steel or glass chamber surface at ambient temperatures, but it is easily desorbed by baking at a temperature above 100 °C for a couple of hours. Baking also adequately reduces the outgassing through diffusion. Permeation of gas through the chamber walls in the case of steel walls is dominated by hydrogen gas that accounts for 90% or more of the pressure built-up due to permeation. The pressure increase due to the hydrogen gas permeation can be realized at a level below the acceptable vacuum-space pressure (0.01 Pa in five years) if the wall thickness is larger than 0.6 mm. In glass chamber, helium gas permeation is the major problem. The pressure in glass vacuum chambers due to helium gas permeation relatively increases quickly to the partial helium gas pressure in the atmosphere (0.52 Pa), which is higher than the acceptable vacuum pressure. A helium gas permeation barrier such as a titanium coating, therefore, is essential. Electrically insulated feedthroughs are available with sufficiently low leak rates. We show that it is possible to maintain a vacuum chamber with above-mentioned volume and inner area at a pressure of maximum 0.01 Pa for five years even without the need of a getter. However, if the materials used in the chamber outgas easily (such as epoxy) or the chamber cannot be baked at sufficiently high temperature (e.g., to prevent damaging of devices inside the chamber), a getter will be needed to compensate for the extra outgassing. In a long-duration experiment with four stainless steel chambers of the above dimensions and equipped with a chemical getter, the vacuum pressures were monitored for a period of two years. In that period, the measured pressure increase stayed within 0.01 Pa. With the developed micro vacuum chamber, a micromachined cryogenic cooler can be realized as a "stand-alone" cooling system without continuous mechanical pumping. Electronic devices can be integrated with a microcooler and placed in such a vacuum chamber.

ACKNOWLEDGMENTS

The authors gratefully acknowledge the support of the Dutch Technology Foundation (STW) under Contract No. 08014 and Kryoz Technologies for partly covering the expenses of the experiment. This work was also supported by NanoNextNL, a micro and nanotechnology consortium of the Government of the Netherlands and 130 partners.

[1]B. Z. Maytal and J. M. Pfotenhauer, *Miniature Joule–Thomson Cryocooling: Principles and Practice* (Springer, New York, 2013).
[2]J. H. Derking, H. J. Holland, T. Tirolien, and H. J. M. ter Brake, Rev. Sci. Instrum. **83**, 045117 (2012).
[3]H. S. Cao, R. H. Witvers, S. Vanapalli, H. J. Holland, and H. J. M. ter Brake, Rev. Sci. Instrum. **84**, 105102 (2013).
[4]H. S. Cao, H. J. Holland, C. H. Vermeer, S. Vanapalli, P. P. P. M. Lerou, M. Blom, and H. J. M. ter Brake, J. Micromech. Microeng. **23**, 025014 (2013).
[5]R. Gooch and T. Schimert, MRS Bull. **28**, 55 (2003).
[6]T. R. Anthony, J. Appl. Phys. **54**, 2419 (1983).
[7]Y. T. Cheng, W. T. Hsu, K. Najafi, C. T. C. Nguyen, and L. W. Lin, J. Microelectromech. Syst. **11**, 556 (2002).
[8]D. R. Sparks, S. Massoud-Ansari, and N. Najafi, Proc. SPIE **5343**, 70 (2004).
[9]D. R. Sparks, S. Massoud-Ansari, and N. Najafi, IEEE Trans. Adv. Packag. **26**, 277 (2003).
[10]J. Mitchell and K. Najafi, *The 15th International Conference on Solid-state Sensors, Actuators and Microsystems* (IEEE, 2009), p. 841.
[11]J. F. O'Hanlon, *A User's Guide to Vacuum Technology* (Wiley, New York, 2003).
[12]P. Danielson, R&D Mag. **43**, 57 (2001).
[13]E. W. Lemmon, M. L. Huber, and M. O. McLinden, Refprop version 8.0, NIST standard reference database 23, Gaithersburg: U.S. Department of Commerce, 2007.
[14]R. Dobrozemsky, J. Vac. Sci. Technol., A **5**, 2520 (1987).
[15]R. Dobrozemsky, Vacuum **46**, 789 (1995).
[16]P. A. Redhead, J. Vac. Sci. Technol., A **13**, 467 (1995).
[17]R. J. Elsey, Vacuum **25**, 299 (1975).
[18]M. Moraw and H. Prasol, Vacuum **49**, 353 (1998).
[19]R. Calder and G. Lewin, Br. J. Appl. Phys. **18**, 1459 (1967).
[20]W. G. Perkins, J. Vac. Sci. Technol. **10**, 543 (1973).
[21]M. R. Louthan, Jr. and R. G. Derrick, Corros. Sci. **15**, 565 (1975).
[22]R. Haberman, *Applied Partial Differential Equations: With Fourier Series and Boundary Value Problems* (Pearson Prentice Hall, NJ, 2003).
[23]W. A. Rogers, R. S. Buritz, and D. Alpert, J. Appl. Phys. **25**, 868 (1954).
[24]S. H. Choa, Microsys. Technol. **11**, 1187 (2005).
[25]Hositrad, Hoevelaken, The Netherlands, see http://www.hositrad.com.
[26]K. M. Welch, J. Vac. Sci. Technol., A **21**, S19 (2003).
[27]A. K. Gupta and J. H. Leck, Vacuum **25**, 362 (1975).
[28]B. Ferrario, A. Figini, and M. Borghi, Vacuum **35**, 13 (1985).
[29]J. M. Lafferty, *Foundations of Vacuum Science and Technology* (Wiley, New York, 1998).
[30]A. Barosi, U.S. patent 3,926,832 (16 December 1975).
[31]A. Barosi and T. A. Giorgi, Vacuum **23**, 15 (1973).
[32]C. D. Park, S. M. Chung, and P. Manini, J. Vac. Sci. Technol., A **29**, 011012 (2011).
[33]MKS Instruments, HPS Products, Boulder, NV, see http://www.mksinst.com.
[34]Saes Pure Gas Inc., San Luis Obispo, CA, see http://www.saespuregas.com.
[35]Y. Tuzi, T. Tanaka, K. Takeuchi, and Y. Saito, Vacuum **47**, 705 (1996).
[36]Y. Shiokawa and M. Ichikawa, J. Vac. Sci. Technol., A **16**, 1131 (1998).